Journal of Physics: Conference Series **3053** (2025) 012004 doi:10.1088/1742-6596/3053/1/012004

Radiation Hardness Assessment and Annealing Strategies for Silicon Photomultiplier Sensors for the Terzina Telescope on-board the NUSES space mission

L. Burmistrov, S. Davarpanah*, M. Heller, T. Montaruli, C. Tönnis, C. Trimarelli for the NUSES Collaboration

Département de Physique Nucléaire et Corpusculaire, Faculté de Genève, Université de Genève, Genève, Switzerland

E-mail: *shideh.davarpanah@unige.ch

Abstract. NUSES is a pathfinder for new satellite platforms developed by THALES and cutting-edge photo sensing technologies, such as SiPM and their associated low-power-consuming electronics. It is financed by the Italian Ministry and conducted by the Gran Sasso Science Institute (GSSI), INFN sections and the University of Geneva. NUSES hosts two payloads: **Ziré** is devoted to low-energy cosmic rays to investigate aspects related to space weather, and gamma-rays from gamma-ray bursts; the **Terzina** telescope will achieve the first observation from space of the Cherenkov light emitted by atmospheric showers induced by ultra-high-energy cosmic rays (UHECRs) within its field of view. Terzina might catch also a few Earth-skimming neutrinos above about 100 PeV. This faint light may only be detected by Terzina from a sun-synchronous orbit at 535 km of altitude while pointing to the limb and viewing the dark side of the earth and atmosphere. In such a configuration, this space-based telescope would not be constrained by the day-night cycle, unlike ground-based Cherenkov telescopes or payloads in non-polar orbit. Terzina is a Schmidt-Cassegrain telescope with dual mirror optics with a 935 mm effective focal length and a primary mirror with a diameter of 430 mm. Its SiPM-based camera is composed of 2 rows of 5 tiles of 8 $\times$ 8 SiPM 3x3 mm^2 pixels. The University of Geneva collaborated with the FBK Research Foundation to define these tiles. We measured in the laboratory the equivalent effect of radiation in space on the SiPM. Understanding the light noise in situ is vital for future larger missions or constellations of such satellites in the plans in the US and Europe and also for other missions employing SiPMs. For this study we utilized a 50 MeV proton beam and a beta-radioactive source of Strontium-90. As a matter of fact, radiation damage increases the DCR, and consequently to keep the signal-to-noise ratio constant the trigger threshold has to be increased. However, we developed an annealing approach suitable for a space-based middle-size satellite to limit the effect of radiation damage while efficiently lowering the SiPM's energy detection threshold.

1 Introduction

Silicon Photomultipliers (SiPMs), also known as Geiger avalanche photodiodes (G-APDs), have emerged as a promising technology for space-based experiments, thanks to their light weight, low power consumption, and excellent photon detection efficiency. These characteristics make SiPMs ideal for detecting faint signals in space. Additionally, their compact size and robustness facilitate their integration into

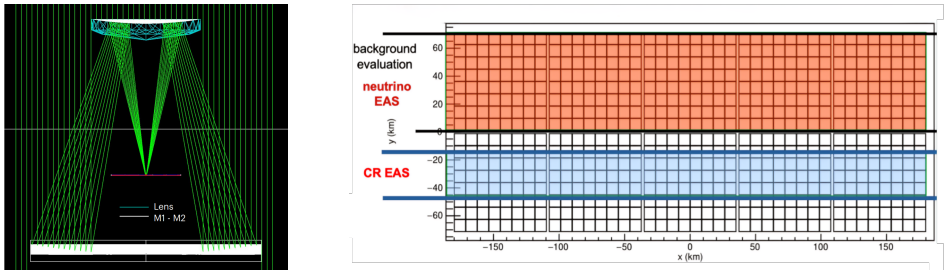

Figure 1: [Left]: A view from the Geant4 simulation of the Terzina Schmidt-Cassegrain telescope with the two mirrors and one corrective lens on top of the second mirror met by the entering light and leading the photons to the camera plane. [Right]: The 10 tiles of the camera plane. Since the optical system of the telescope will give an upside-down image and left-to-right flip therefor any events coming from above the Earth's limb will show on the lower row of the camera plane and vice versa.

lightweight and compact space instruments. However, SiPMs face challenges such as sensitivity to temperature variations and susceptibility to radiation-induced damage increasing the already high dark count rate (DCR). While very high temperature (beyond 80 °C) and high-gradients of temperature variation can affect their immediate performance, radiation damage can degrade their performance over time. This necessitates meticulous behavior studies and strategies to maintain as possible their reliability in the harsh conditions of space. These strategies are relevant because SiPMs could contribute significantly to our understanding of the universe and the advancement of space-based scientific discoveries from space.

Ongoing research and development aim to mitigate these challenges and improve the performance of SiPMs in space applications. Despite their limitations, SiPMs hold significant potential for advancing space exploration by enabling the detection of UHECRs and neutrinos. The NUSES (Neutrinos and Seismic Electromagnetic Signals) space mission [1], hosting two payloads: Terzina [2] and Zirè [3], exemplifies the SiPMs application. Operating in a quasi-polar Low Earth Orbit, NUSES aims to explore new scientific and technological pathways for astro-particle physics detectors.

The Terzina camera is designed to detect Cherenkov light from extensive air showers induced by UHECRs with its lower part and the upper part will target the dark side of the Earth's limb to detect earth-skimming neutrino events (see Fig. 1). As a matter of fact, the optics reverses images. The optical axis of the telescope is inclined at 67.5° with respect to the nadir pointing at the limb. By capturing a small part of the tens ok kilometer wide Cherenkov light cone from UHECRs and neutrinos, Terzina aims to achieve high exposure to these rare phenomena.

This paper is structured as follows: Sec. 2 provides an in-depth description of the Terzina Cherenkov telescope, detailing its design and target events. Sec. 3 examines the background radiation in space and its potential impact on the mission. In Sec. 4, we present the measurement techniques used to assess the SiPM response, including the results from the proton and electron irradiation campaign, the subsequent calculation of the DCR, and the annealing processes. Finally, we conclude with a discussion of the results and their implications for future space missions in the last section.

2 The Terzina Cherenkov telescope

The Terzina detector consists of a near-UV optical telescope featuring Schmidt-Cassegrain optics and a Focal Plane Assembly (FPA), as illustrated in Fig. 1. The optical unit includes a dual mirror system with an effective focal length of 935 mm and a primary mirror with a 454 mm diameter. The FPA, which is made up of two rows of five tiles each containing 8×8 SiPM pixels measuring $3{\times}3$ mm^2, is designed to detect photons from below (mainly to characterize the background) and from above the horizon (to observe Extensive Air Shower (EAS) generated by cosmic rays) and it will be the very first observation of Cherenkov signal from space. Each pixel has a 0.18° point of view, resulting in a 7.2° field of view along the Earth's horizon and 2.9° across it. The Terzina camera plane [4] will use NUV-HD-MT SiPMs produced by FBK [5], featuring NUV-HD technology that incorporates metal-filled Deep Trench Isolation (DTI) to significantly reduce optical cross-talk (between $0 - 10\%$ up to 10 V over-voltage).

Terzina is specifically designed to detect Cherenkov light emitted by EAS induced by UHECRs and neutrinos in the Earth's atmosphere. There are two categories of target events: UHECRs with energies above 100 PeV coming from the top of the atmosphere and induce downgoing showers; and the tau and muon neutrinos with energies above few PeV passing through the Earth can produce τ and μ leptons,

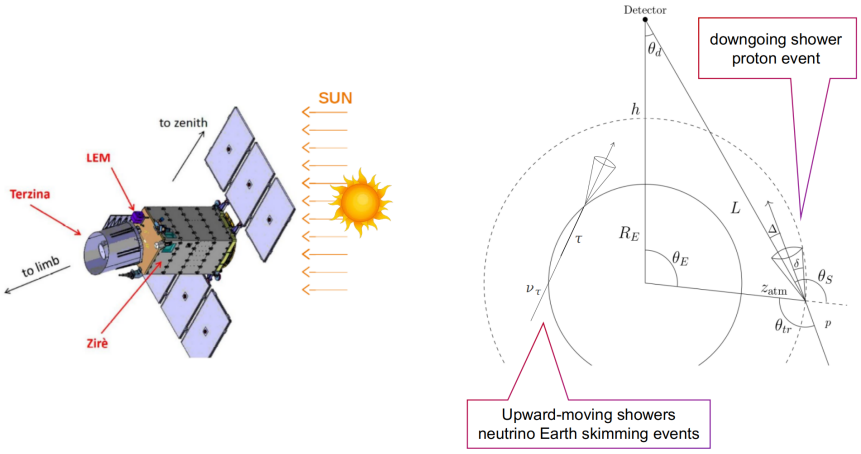

Figure 2: [Left]: the general scheme of the NUSES satellite design. [Right]: Target events of the Terzina Cherenkov telescope with a proton-induced downgoing shower on the right and an upgoing shower produced by a tau neutrino Earth-skimming event on the left, based on [6].

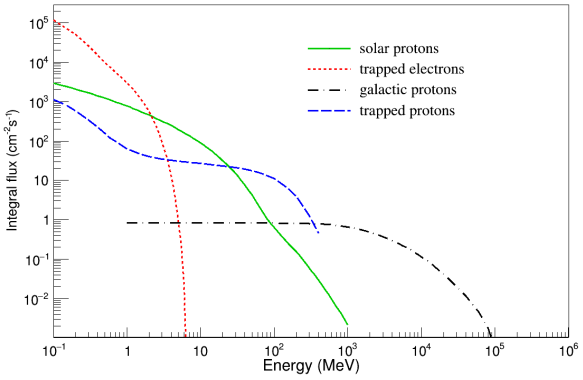

Figure 3: Integrated fluxes of trapped electrons and protons in the Van Allen Belts, solar protons, and galactic protons over the 3-year duration of the NUSES mission in its quasi-polar Low Earth Orbit, reported as the average per second. Note that without averaging, solar protons will show higher instantaneous spikes in flux as their occurrence is not continuous.

which can emerge in the atmosphere from the Earth, generating upgoing EAS (Earth skimming neutrinos), illustrated in Fig. 2.

3 Background radiation in space

The atmosphere significantly reduces the arrival of background radiation on ground thanks to processes such as absorption on different elements and multiple scattering. However, the Terzina telescope, positioned in a low Earth orbit (LEO) at an altitude of 535 km and a high inclination of approximately 97.8°, is not shielded by the atmosphere. It primarily receives radiation from Solar Particle Events (SPEs), trapped protons and electrons within the Van Allen Radiation Belts, and galactic cosmic rays (GCRs). By utilizing SPENVIS (Space Environment Information System) [7] software, we can plot the expected flux from all of these sources over the mission's duration—from mid-2026 (launch time and beginning of life) to mid-2029 (end of life). Figure 3 indicates that the dominant fluxes originate from trapped electrons, trapped protons, and solar protons, so further analysis will focus on these three sources.

As mentioned these fluxes will be a source of irradiation and consequently of increased noise for the Terzina camera plane. The irradiation dose received by the SiPM array will cause atom displacements within the SiPM lattice. Over time, these displacements form regions with higher concentrations of silicon,

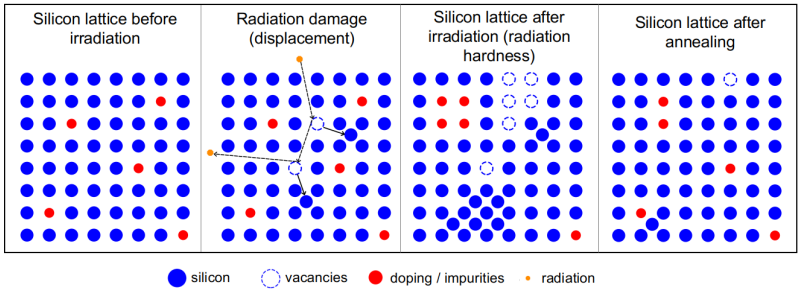

Figure 4: An example of the SiPMs lattice at the atomic scale in 2-dimension starting with almost even spacing between doping or impurities (far left), during irradiation (middle left), and the resulting radiation hardening (middle right). On the far right, there is an example of the same lattice after the annealing procedure.

impurities or doping materials, and vacancies. When clusters of such vacancies and silicon form, these regions become less flexible, which increases the dark count rate of the SiPM, thereby reducing image quality and increasing the event acceptance energy threshold. One method to address this issue, known as radiation hardness, involves heating the SiPM lattice. The increased kinetic energy of the atoms helps reorder their positions in the lattice, partially restoring the SiPMs' original physical properties, though not completely. In space, some of the ways in which this heating treatment, called annealing, can be performed are by applying a direct bias to generate a high current through the SiPMs, illuminating the tiles with LEDs, or adding heaters to the PCB (e.g., by placing resistors behind the PCB). For Terzina, the chosen method is to add the resistors and conduct annealing in a periodic cycle to maximize efficiency. The annealing limits the increase of the DCR, then of the trigger threshold. In the ideal case of a complete recovery of the radiation damage, the threshold would stay the same. The processes of radiation hardness and annealing at the atomic scale are illustrated in Fig. 4.

4 SiPM response measurement

We developed an experimental setup to measure the current-voltage curve (IV curve) of the SiPMS while irradiated with protons and electrons. For this purpose, we use the NUV-HD-MT SiPM produced by FBK [5] of 3×3 mm^2 and 1×1 mm^2 and 40 μm and 30 μm cell sizes respectively and the measuring devices are Keithley 2400 [8] and 6487 [9] pico-ammeter/voltage source I−V for bias supply and current measurements. All the laboratory measurements are performed at room temperature on average $T = 22°C$ and the results are reported for 10 V over-voltage.

4.1 Irradiating the SiPMs

We measured the current of the SiPMs as a function of their bias voltages in the post-breakdown Geiger regime, in two different irradiation cases as follows:

- *Proton irradiation:* We performed the first proton irradiation test at IFJ PAN in Krakow [10] with a 50 MeV proton beam. The proton beam spot had a circular shape with a 35 mm diameter and homogeneity better than 5% with respect to the mean fluence. We measured the currents for the 1×1 mm^2 and 30 μm cell size SiPM with resin coating.
- *electron irradiation:* We utilize strontium 90, a beta emitter, the 3×3 mm^2 and 40 μm cell size SiPM with resin coating. The isotope Strontium 90 with an atomic number of 38 and a half-life of about 28.8 years exclusively undergoes beta decay, with a decay energy of 0.546 MeV, into yttrium-90 and produces an electron and a neutrino. Yttrium-90 (Y90) with a half-life of 64.2 hours also beta decay to stable zirconium (Zr). With this source, we can study the SiPM radiation damage from electrons up to the maximum energy of 2.2 MeV.

On the other hand, considering the fluxes on Fig 3, we use Geant4 [11, 12, 13], a toolkit for simulating the passage of particles through matter, to estimate the non-ionizing dose expected on the Terzina camera with the exact geometry of the telescope and estimate the expected non-ionizing dose per time for one

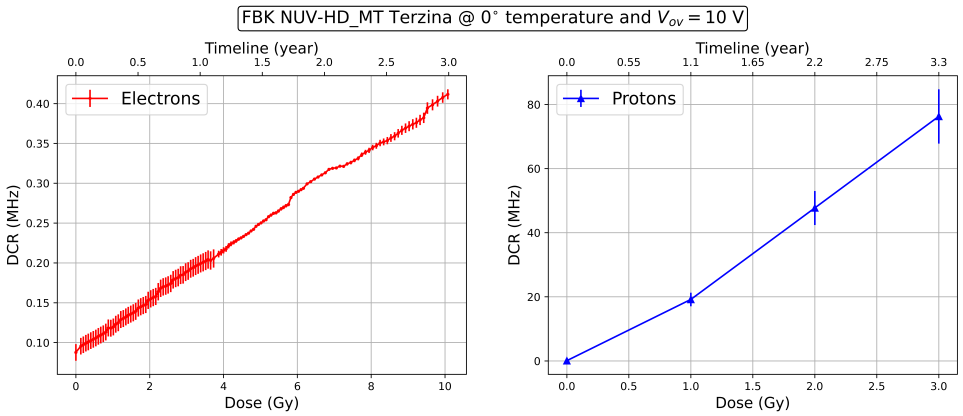

Figure 5: Inferred DCR per pixel for Terzina SiPMs sensitive area ~ 6.58 mm^2 from IV measurements during the irradiation as a function of dose and mission timeline.

SiPM pixel. We obtained 10.1 Gy[1]/year for electrons and 2.7 Gy/year for protons.

4.2 DCR calculation

The DCR represents the baseline count rate in the absence of incident light, defining the minimum threshold where photon-induced signals are detectable. Consequently, higher DCR values increase the detector's readout threshold, impacting the lowest achievable energy resolution. With the current measurements, we can now calculate the DCR using the following formula:

$$\mathrm{DCR}(10\,\mathrm{V_{ov}}, \mathrm{dose}) \propto \frac{I(10\,\mathrm{V_{ov}}, \mathrm{dose})}{\mathrm{Gain}\,.\,q\,.\,s^*} \times \frac{\text{sensitive area}}{T_{\mathrm{factor}}}, \qquad s^* = \begin{cases} 1\ \mathrm{mm}^2 & \text{for } 1\times 1 \text{ SiPM} \\ 9\ \mathrm{mm}^2 & \text{for } 3\times 3 \text{ SiPM} \end{cases} \tag{1}$$

Here, the I, Gain, T_{factor}, dose, and q stand for the measured currents, gain of the SiPM in use, the temperature conversion factor from 22.0°C to 0°C, the dose from the source in use, and the electron charge respectively. The s^* is the factor to convert the current from the SiPM in use to one pixel. Combining the DCR results with the dose-per-time ratio from the simulation yields the results in Fig. 5.

4.3 Annealing

In the laboratory, we perform annealing by placing the devices in a climatic chamber at a fixed temperature for a certain period and regularly measuring the IV curve. By comparing the new current with the SiPM's current before irradiation at a given over-voltage, we determine the recovery efficiency of the annealing cycles. Based on various measurements for different SiPMs at fixed temperatures, we concluded that at temperatures above 50°C and an annealing cycle of 84 hours, up to 40% of the SiPM's response current can be recovered. Using this information, we constructed a model for the DCR change over time for space applications. The two components that change the DCR during the mission are the annealing cycle and the irradiation cycle. The annealing cycle reduces the DCR exponentially, while the irradiation cycle increases it linearly. Note that over time, the effectiveness of annealing cycles decreases as the lattice becomes more rigid and less responsive to the heating treatment. The resulting DCR from proton irradiation as a function of time or dose for three different annealing cycles is shown in Fig. 6.

5 Conclusion

Overall, from Fig. 5, we can see that, as expected, electrons cause at least two orders of magnitude smaller change in the DCR compared to protons, despite the much higher fluence of trapped electrons, especially low-energy electrons, compared to trapped and solar protons. Figure 5 provides a clear expectation of the annealing results in space and the anticipated noise levels. This information allows us to adjust the trigger energy threshold throughout the 3-year mission to optimize the observation of Cherenkov signals, ensuring the best signal-to-noise ratio.

[1] 1 rad = 0.01 Gy = 0.01 J/kg

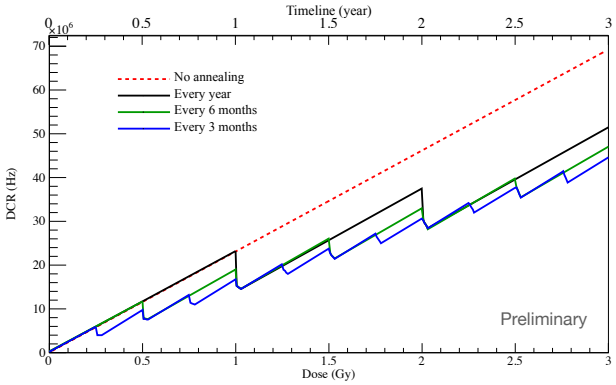

Figure 6: The DCR change from the proton irradiation and annealing cycles during the satellite lifetime.

Acknowledgement
This work was made possible thanks to an excellence PhD fellowship of the Swiss Confederation.

References

[1] Trimarelli C. The NUSES space mission. PoS. 2024;TAUP2023:121.
[2] Burmistrov L. Terzina on board NUSES: A pathfinder for EAS Cherenkov Light Detection from space. EPJ Web of Conferences. 2023;283:06006. http://dx.doi.org/10.1051/epjconf/202328306006 and https://arxiv.org/abs/2304.11992.
[3] De Mitri I, Fernandez Alonso M. The Zire experiment on board the NUSES space mission. PoS. 2023;ICRC2023:139.
[4] Burmistrov L. A Silicon-Photo-Multiplier-Based Camera for the Terzina Telescope on Board the Neutrinos and Seismic Electromagnetic Signals Space Mission. Instruments. 2024;8(1). Available from: https://www.mdpi.com/2410-390X/8/1/13.
[5] Gola A, Acerbi F, Capasso M, Marcante M, Mazzi A, Paternoster G, et al. NUV-Sensitive Silicon Photomultiplier Technologies Developed at Fondazione Bruno Kessler. Sensors. 2019;19(2). Available from: https://www.mdpi.com/1424-8220/19/2/308.
[6] Cummings AL, Aloisio R, Eser J, Krizmanic JF. Modeling the optical Cherenkov signals by cosmic ray extensive air showers directly observed from suborbital and orbital altitudes. Phys Rev D. 2021 Sep;104:063029. https://link.aps.org/doi/10.1103/PhysRevD.104.063029 and https://doi.org/10.48550/arXiv.2105.03255.
[7] SPENVIS: The Space Environment Information System; 2022. Accessed on June 12, 2024. Available from: https://www.spenvis.oma.be/.
[8] Manual U. Series 2400 SourceMeter; 2011. https://download.tek.com/manual/2400S-900-01_K-Sep2011_User.pdf.
[9] Manual U. Series 6487 SourceMeter; 2011. https://download.tek.com/manual/6487-901-01(B-Mar2011)(Ref).pdf.
[10] Swakon J, Olko P, Adamczyk D, Cywicka-Jakiel T, Dabrowska J, Dulny B, et al. Facility for proton radiotherapy of eye cancer at IFJ PAN in Krakow. Radiation Measurements. 2010;45(10):1469-71. PROCEEDINGS OF THE 11TH SYMPOSIUM ON NEUTRON AND ION DOSIMETRY. Available from: https://www.sciencedirect.com/science/article/pii/S1350448710002118.
[11] Allison J, Amako K, Apostolakis J, Arce P, Asai M, Aso T, et al. Recent developments in Geant4. Nuclear Instruments and Methods in Physics Research Section A: Accelerators, Spectrometers, Detectors and Associated Equipment. 2016;835:186-225. Available from: https://www.sciencedirect.com/science/article/pii/S0168900216306957.
[12] Allison J, Amako K, Apostolakis J, Araujo H, Arce Dubois P, Asai M, et al. Geant4 developments and applications. IEEE Transactions on Nuclear Science. 2006;53(1):270-8.
[13] Agostinelli S, Allison J, Amako K, Apostolakis J, Araujo H, Arce P, et al. Geant4—a simulation toolkit. Nuclear Instruments and Methods in Physics Research Section A: Accelerators, Spectrometers, Detectors and Associated Equipment. 2003;506(3):250-303. Available from: https://www.sciencedirect.com/science/article/pii/S0168900203013688.